

Observation of Coulomb Blockade Oscillations up to 50K from InP-Based InGaAs Quantum Wires Grown by Molecular Beam Epitaxy

Hiroshi OKADA, Hajime FUJIKURA, Tamotsu HASHIZUME and Hideki HASEGAWA

Research Center for Interface Quantum Electronics and Graduate School of Electronics and Information Engineering, Hokkaido University, Sapporo 060, Japan

Phone: +81-11-706-7174, Fax: +81-11-716-6004

E-mail: okada@ryouko.rciqe.hokudai.ac.jp

InP-based quantum wire transistors were successfully fabricated for the first time directed on InAlAs/InGaAs ridge quantum wires (QWRs) grown by selective MBE. Each wire showed strong photoluminescence, cathodoluminescence and Shubnikov-de Haas (SdH) oscillations. Behavior of SdH oscillation confirmed presence of one-dimensional transport. QWR transistor showed clear Coulomb blockade oscillations near pinch-off up to 50K. Coulomb gap was estimated to be 24mV. Possible mechanisms for dot formation are discussed.

1. Introduction

A practical manufacturing technology of single electron transistors (SETs) should be capable of producing, within an acceptable turn-around time, an extremely high density of small-enough and defect-free quantum dots with acceptable uniformity and yields. III-V compound semiconductor technologies, particularly InP-based technologies, seem to be promising due to wide ranges of material selection for optimal potential design, large values of conduction band offsets, superb electron transport, high-precision epitaxy techniques and availability of selective and self organized growth modes for defect-free nanostructures. However, compound semiconductor SETs reported so far are GaAs-based split-gate devices which operate only in the mK range.

In this paper, an InP-based InGaAs quantum wire (QWR) transistor was successfully fabricated for the first time, directly on to an well-behaved ridge QWR grown by selective molecular beam epitaxy. Clear Coulomb blockade oscillations were observed up to 50 K near pinch-off.

2. Device Structure and Fabrication Process

The structure of the QWR transistor is shown in Fig. 1. An InAlAs/InGaAs ridge quantum wire is used as the channel. In this transistor, the current through the wire is supplied by the source and drain ohmic contacts and is controlled by the Schottky gate.

The device fabrication process consisted of selective-MBE growth of the QWR wafer and standard photolithography processes to form ohmic and Schottky contacts to the wires. The cross section of the QWR

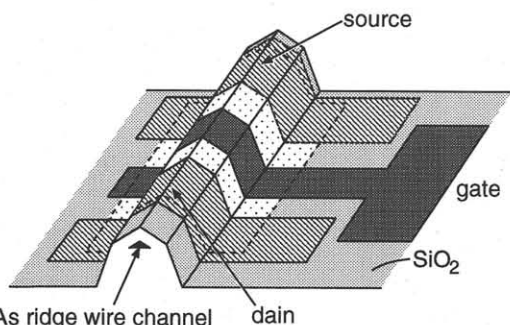


Fig. 1: Schematic view of quantum wire transistor structure.

wafer used in this study which contains array of the InAlAs/InGaAs wires is schematically shown in Fig. 2. Details of such wire formation by selective MBE growth were presented elsewhere¹⁾. Briefly, mesa stripes toward $\langle 110 \rangle$ direction with $4\mu\text{m}$ pitch were formed by standard photolithography and wet etching on (001) semi-insulating InP substrates. Then, a thick InGaAs buffer layer was grown, resulting in formation of (311)A facets on the top. A subsequent InAlAs growth then modifies the top to become (411)A facets, onto which a thin InGaAs layer was grown. This realizes arrow-headed QWRs bounded by (311) and (411) facets at the ridges. Then the top InAlAs barrier was grown. Carrier supply to the wire was achieved by Si-doping into the top InAlAs layer after growth of an undoped-InAlAs spacer layer. As the cap layer, Si-doped thin InGaAs layer was grown. The entire structure was then covered with a photo-CVD SiO₂ layer for further photolithography processing.

After the growth of the QWR wafer, SiO₂ windows were opened for selective formation of ohmic contacts to QWRs. Then, source and drain Au/Ge/Ni ohmic electrodes were formed by lift-off process followed by alloying at 350°C for 2 minutes in H₂ atmosphere. Finally, Pt/Au Schottky gate electrodes were formed by lift-off process. Channel length between source and drain ohmic contacts was $7\mu\text{m}$ and the gate length was $4\mu\text{m}$.

3. Results and Discussion

3.1 SEM and Optical Characterization of InGaAs wires

An example of SEM micrograph showing the cross section of the wire region is shown in Fig. 3(a). Formation of an arrow-headed wire with a width of 100nm is clearly seen. The SEM plan view of the QWR wafer is given in Fig. 3(b). The surface of the wafer was found

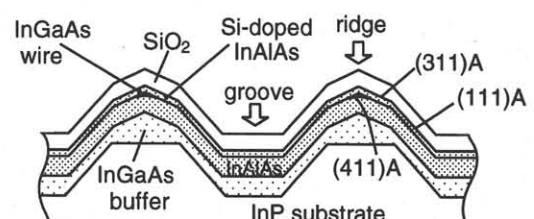


Fig. 2: Cross section of QWR wafer.

to be extremely smooth in the ridge region, whereas the structure was rather irregular in the bottom groove region.

The QWR array gave strong cathodoluminescence (CL) and photoluminescence (PL). Monochromatic CL study confirmed that the luminescence comes from the QWR itself as shown in Fig. 4. The PL spectrum observed from the QWR array is shown in Fig. 5. PL was observable up to room temperature.

3.2 Magneto-transport properties of InGaAs wires

Each wire showed clear Shubnikov-de Haas (SdH) oscillations in the two-terminal configuration at 4.2K in the dark, as shown in Fig. 6.

From the SdH oscillations, the Landau index N

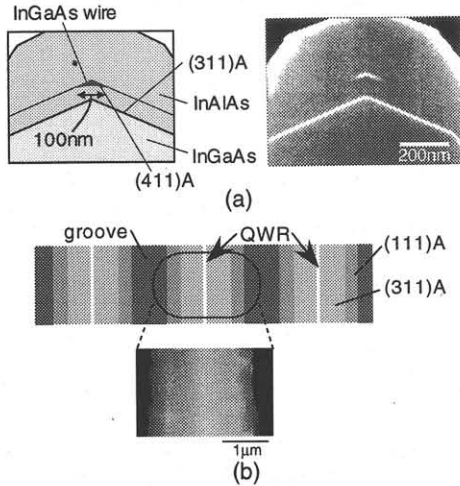


Fig. 3: (a)Cross section and (b)plan view of QWR.

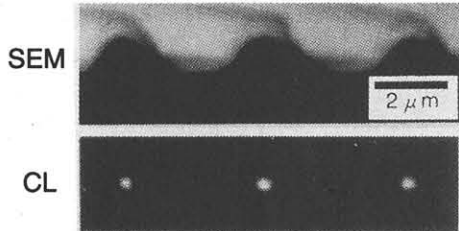


Fig. 4: Monochromatic CL image of QWR.

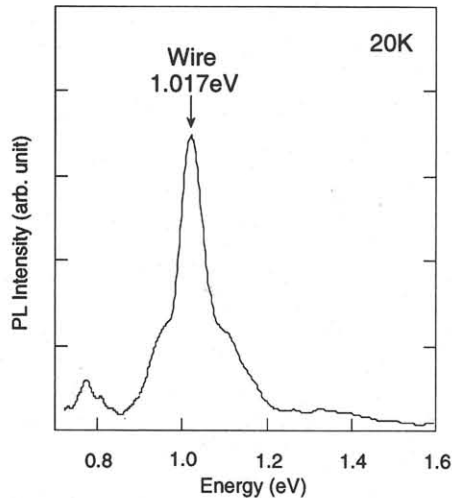


Fig. 5: PL spectrum of QWR.

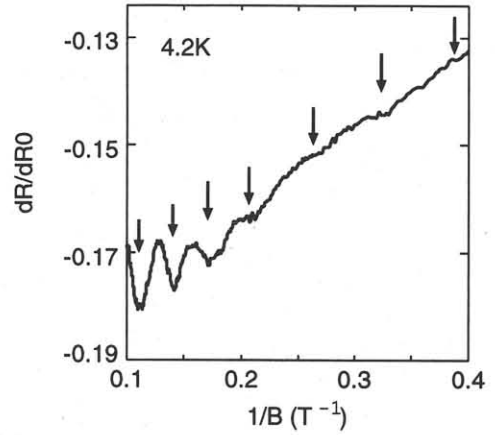


Fig. 6: Magnetoresistance oscillation at 4.2K.

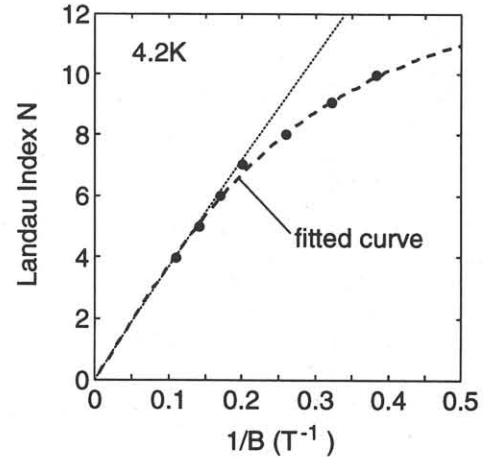


Fig. 7: Landau plot.

were determined and plotted vs. the inverse of magnetic field $1/B$, as shown in Fig. 7. As seen in Fig. 7, a non-linear relationship appears between N and $1/B$ at about or below 5T, indicating on-set of one-dimensional transport. Fitting the data to a theoretical curve based on the parabolic potential approximation as shown in Fig. 7, a zero bias wire width of 95nm, linear electron density of $1.6 \times 10^7 \text{cm}^{-1}$ and an energy level spacing of 10meV were obtained. This value of the level spacing is much larger than the values of 1–3meV typically found for GaAs-based split-gate wires. Thus, a much stronger confinement potential is realized in the present QWR. The estimated wire width of 95nm is in excellent agreement with that obtained by the cross-sectional SEM observation.

3.3 Electrical Characteristics of QWR Transistor

The fabricated QWR transistor showed good drain current–voltage characteristics with an excellent gate control. It was also found that they showed clear and reproducible Coulomb blockade oscillations near pinch-off as shown in Fig. 8. The Coulomb blockade oscillation was observable at least up to 50K, although the gate leakage currents masked the traces of the Coulomb blockade oscillations.

Presence of Coulomb blockade behavior was also confirmed in the drain I – V characteristics, as shown in Fig. 9. From Fig. 9, the value of Coulomb gap was es-

timated to be 24mV. Presence of such a large Coulomb gap is consistent with the observation of Coulomb blockade oscillations up to high temperatures.

To further investigate the Coulomb blockade characteristics, the second derivatives of the drain currents were plotted vs. drain-source voltage V_{ds} in Fig. 10 for the gate voltages from -1.82V to -2.2V . The curves were off-set for clarity. The valley and peak positions indicated by short bars, produce a diamond shaped chart, as indicated by dashed guide lines. Asymmetry of the diamond shape suggests that the potential barriers are asymmetric on both ends of the quantum dot. The area of diamond shape is increased with increasing the negative gate bias voltage, indicating that the size of the dot is changed through the gate bias.

The origin of the Coulomb blockade characteristics observed in our QWR transistor is not clear yet. Si- and GaAs-based QWRs have been reported to show Coulomb blockade oscillations observable up to 100mK range^{2,3)} due to segment formation by random potential of the doped impurity atoms. The present Coulomb blockade oscillation cannot be explained by such mechanism, since it goes up to 50K. The present result seems to be similar to recently reported high-temperature Coulomb blockade oscillation from a Si-QWR transistor⁴⁾ where inhomogeneous oxidation near the wire

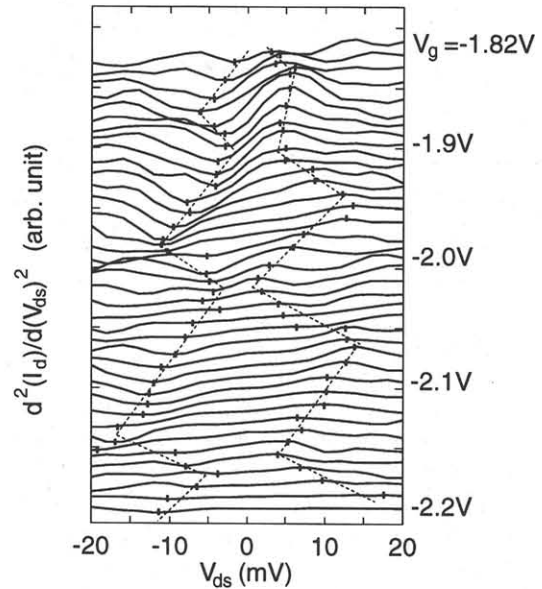


Fig. 10: The second derivative of the drain current vs. drain-source voltage. Short bars indicate the valley and peak position. The dashed line gives guide for eyes.

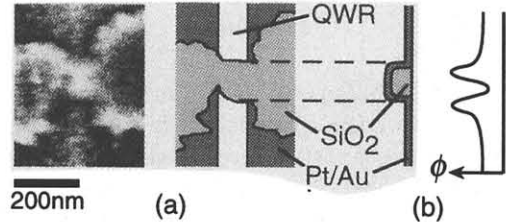


Fig. 11: Model for dot formation. (a) SEM micrograph of SiO_2 residue on the QWR channel and (b) fluctuated potential distribution.

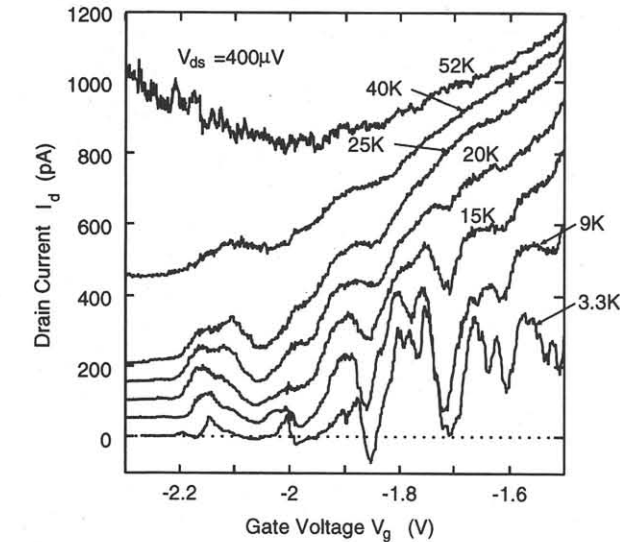


Fig. 8: I_d - V_g characteristic at various temperatures.

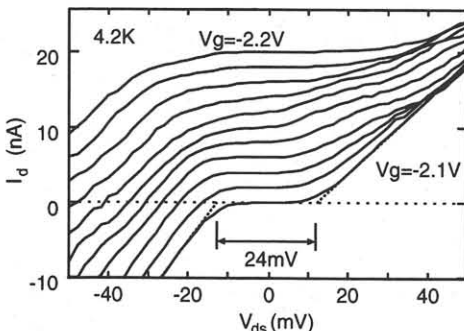


Fig. 9: I_d - V_{ds} characteristic at 4.2K

edges has been reported to be the reason for dot formation. In the present study, a more detailed SEM observation of the wire revealed presence of a SiO_2 residue on the top of the QWR, as shown in Fig.11(a). Thus, one possible mechanism for dot formation is through potential modulation shown in Fig. 11(b) caused by such a residue. The result strongly indicates that combination of the precise epitaxial growth technology with the standard EB lithography to realize artificial Schottky or MIS potential modulation to well-behaved uniform QWR arrays may be a very promising approach for realization of high-temperature operating compound semiconductor single electron devices and their integrated circuits.

References

- 1) H. Fujikura and H. Hasegawa: J. Electron. Mater. **25** (1996) 619.
- 2) J. H. F. Scott-Thomas, S. B. Field, M. A. Kastner, H. I. Smith and D. A. Antoniadis: Phys. Rev. Lett. **62** (1989) 583.
- 3) A. A. M. Staring, H. van Houten, C.W.J. Beenakker and C. T. Foxon: Phys. Rev. B **45** (1992) 9222.
- 4) Y. Takahashi, M. Nagase, H. Namatsu, K. Kurihara, K. Iwade, Y. Nakajima, S. Horiguchi, K. Murase and M. Tabe: Technical digest of IEDM 94 (1994) 938.